# Charge and Wavelength Scaling of RF Photoinjector Designs

J. Rosenzweig
*UCLA Department of Physics*
*405 Hilgard Ave., Los Angeles, CA 90024*

E. Colby
*UCLA Department of Physics and*
*Fermi National Accelerator Laboratory*
*P.O. Box 500, Batavia, IL 60510*

March 6, 1995

## Abstract

The optimum design of an emittance compensated rf photoinjector is very complicated and time-consuming, relying heavily on multi-particle simulations without good analytical models as a guide. Emittance compensated designs which have been developed, however, can be used to generate other designs with no additional effort if the original design is scaled correctly. This paper examines the scaling of rf photoinjector design with respect to charge and wavelength, and presents emittance and brightness scaling laws for these variables. Parametric simulation studies are presented to illustrate these scaling laws. Deviations from scaling and practical considerations are also discussed.

To be published in the *Proceedings of the Advanced Accelerator Workshop,*
Lake Geneva, Wisconsin, June 1994.

## INTRODUCTION

The optimization of an rf photoinjector[1-6] design is typically an iterative and somewhat haphazard process. This is because, while some scaling laws concerning photoinjector performance have been derived from first order integration of the transverse force equations[2], an optimized photoinjector will necessarily use emittance compensation[3], which is a dynamical process with only a qualitative theoretical understanding. A full design therefore requires a search of the relevant parameter space, which includes the rf amplitudes of the gun and booster linac, the focusing lens position and strength, the gun-to-linac separation, the initial gun cell length, as well as the beam charge, spot size and pulse length. Because this is such an involved process, including detailed rf and magnet design calculations and multiparticle simulations (*e.g.* from.PARMELA) any analytical understanding of the optimization process would be very useful and time-saving tool. While a full dynamical theory of the beam dynamics in an rf photoinjector remains a difficult and perhaps remote result, this paper presents a powerful analytical method, that of scaling an existing rf photoinjector design with respect to charge and wavelength variation to predict the performance of entire families of photoinjectors.

## DYNAMICS EQUATIONS

The longitudinal and transverse dynamics of the electrons in an rf photoinjector can be described by some relatively straightforward equations. Since the longitudinal motion is dominated by the applied rf fields, and the collective effects due to the electrons are perturbations on the motion of a single electron, for the purpose of this discussion it is sufficient to examine the single particle dynamics. The rf acceleration field in a $\pi$-mode standing wave accelerator gives an energy gain equation, ignoring spatial harmonics higher than the fundamental, of the form[2]

$$\frac{d\gamma}{dz} = \frac{eE_0}{2m_e c^2}\left[\sin(\phi) + \sin(\phi + 2k_z z)\right], \tag{1}$$

where $k_z = \omega/c$ is the longitudinal rf wave number, and $E_0$ is the peak acceleration field. The phase angle $\phi = k_z z - \omega t + \phi_0$ is defined relative to the forward (accelerating) component of the standing wave, and its evolution is described by

$$\frac{d\phi}{dz} = k_z\left(1-\beta^{-1}\right) = k_z\left[1-\frac{\gamma}{\sqrt{\gamma^2-1}}\right]. \tag{2}$$

A search for a scalable quantity in these Eqs. 1 and 2 is not difficult; by recasting the equations using the dimensionless independent variable $\tilde{z} \equiv k_z z$,

$$\frac{d\gamma}{d\tilde{z}} = \alpha\left[\sin(\phi)+\sin(\phi+2k_z z)\right] \tag{3}$$

$$\text{and } \frac{d\phi}{d\tilde{z}} = \left[1-\frac{\gamma}{\sqrt{\gamma^2-1}}\right], \tag{4}$$

where $\alpha \equiv eE_0/2k_z m_e c^2$ is the single parameter[2] which describes the longitudinal motion of the electron in the applied field. This immediately gives the result that the scaling of an rf design with wavelength implies that $\alpha$ must be kept constant as the wavelength is varied. We will elaborate on this point below.

The transverse dynamics of an optimized rf photoinjector are a bit more intricate to describe, because the collective forces due to space-charge are non-negligible throughout the device. In fact, the uncorrelated thermal motion (thermal emittance) of the beam particles is in fact nearly ignorable in optimized rf photoinjectors because of the dominance of space charge and externally applied forces. This situation allows a key simplification in modeling the collective transverse dynamics, that the motion can be assumed to be nearly laminar. In other words, particle trajectories do not cross. An ordering of particles in the transverse (as well as longitudinal) coordinates is well preserved in this case.

Given this situation, assuming the configuration space distribution functions of the beam at the cathode are the scaled correctly, the scaling of the transverse motion of all of the electrons can be deduced by examining the scaling behavior of the rms transverse envelope equations. For the purpose of this work, we write only the envelope equation describing the evolution of a cylindrically symmetric beam, in the absence of thermal emittance effects[7],

$$\sigma_x'' + \sigma_x'\left(\frac{(\beta\gamma)'}{\beta\gamma}\right) + K_x\sigma_x = \frac{2I}{I_0(\beta\gamma)^3\sigma_x} f\left(\frac{\sigma_x}{\beta\gamma\sigma_z}\right), \tag{5}$$

where an analogous equation exists for $\sigma_y$ (and in fact for $\sigma_z$, which could be used to rigorously replace the discussion of longitudinal dynamics leading to Eqs. 1-4). In Eq. 5 the prime indicates the derivative with respect to $z$, the focusing strength (which is the square of a betatron wave number) $K_x \equiv k_\beta^2 = -F_{ext}/\beta^2\gamma m_e c^2 x$ for all linear static externally applied forces, $I$ is the peak current, and $I_0 \approx 17$ kA is the Alfven current.

## CHARGE SCALING

Often, one designs an rf photoinjector with a particular application in mind, specifying the charge $Q$, bunch length $\sigma_z$, and total (including nonthermal sources) emittance $\varepsilon$, only to find another significantly different application arising later. An example of this occurred during the design of an rf photoinjector for the TESLA Test Facility[8], which is a high charge and emittance device ($Q = 8$ nC, $\varepsilon < 10$ mm-mrad). The potential application of the TTF for creating a beam for a short wavelength free-electron laser (FEL) entered into consideration some time after the emittance compensated design for the high charge case had matured. The natural question came to mind when the FEL application arose as to whether a low emittance and charge beam could be produced by the same device. This initiated our study of charge, or $Q$ scaling.

An rf photoinjector design can be scaled quite straightforwardly by scaling the defocusing forces of the bunch appropriately. This can be seen by writing $I = Qc/g\sigma_z$, where $g$ is a distribution function dependent form factor, and using the defocusing space charge term in Eq. 5 to define the rms defocusing (imaginary) wave number as

$$K_{sc} = \kappa_{sc}^2 = \frac{2I}{I_0(\beta\gamma)^3\sigma_r^2} f\left(\frac{\sigma_x}{\beta\gamma\sigma_z}\right) = \left[\frac{2c}{I_0\beta^2\gamma^3}\right]\left[\frac{Q}{g\sigma_z\sigma_x^2}\right] f\left(\frac{\sigma_x}{\beta\gamma\sigma_z}\right). \qquad (6)$$

The first bracketed factor in Eq. 6 is a bunch independent constant, the second is, up to a distribution shape dependent constant, the peak beam density, and the last factor is dependent only on the bunch aspect ratio. Therefore one can scale a design keeping all of the applied focusing forces the same by preserving the defocusing space charge wave number, which implies that peak the beam density, aspect ratio and distribution shape must be kept constant. Quantitatively we can write this as a simple scaling law,

$$\sigma_i \propto Q^{1/3}, \qquad (7)$$

all bunch dimensions must be scaled as the cube-root of the total charge.

To check on how well this scaling works in actual practice, a series of simulations were performed using the code PARMELA, which includes all applied fields and an electrostatic approximation to the self-consistent space charge fields. A test injector composed of a high gradient 1-1/2 cell S-band (2856 MHz) photoinjector gun with BNL-style cavity profiles[4], followed by a focusing solenoid (with associated a bucking coil) approximately 1.5 RF wavelengths long, and a drift long enough to allow the compensation minimum to be clearly discerned was chosen for the scaling studies. No effort was made to match the compensated beam into a subsequent linac section. A cylindrically symmetric charge distribution, both radially and longitudinally uniform, was assumed. "Guard charge" (amounting to 25% additional charge over the desired final value) was used to help preserve the linearity of the space charge force at the outer edge of the beam core, and was collimated away to compute the beam emittances. Rf cavity fields were derived from a Fourier-Bessel expansion. Although the optimal launch phase for minimum emittance changes for differing bunch charges owing to the variation in the longitudinal and transverse space charge effects of the image charge at the cathode (which do not scale the same as the beam-s self-space charge), the launch phase was not optimized for each case, rather the optimal launch phase for the 1 nC case was used for all cases.

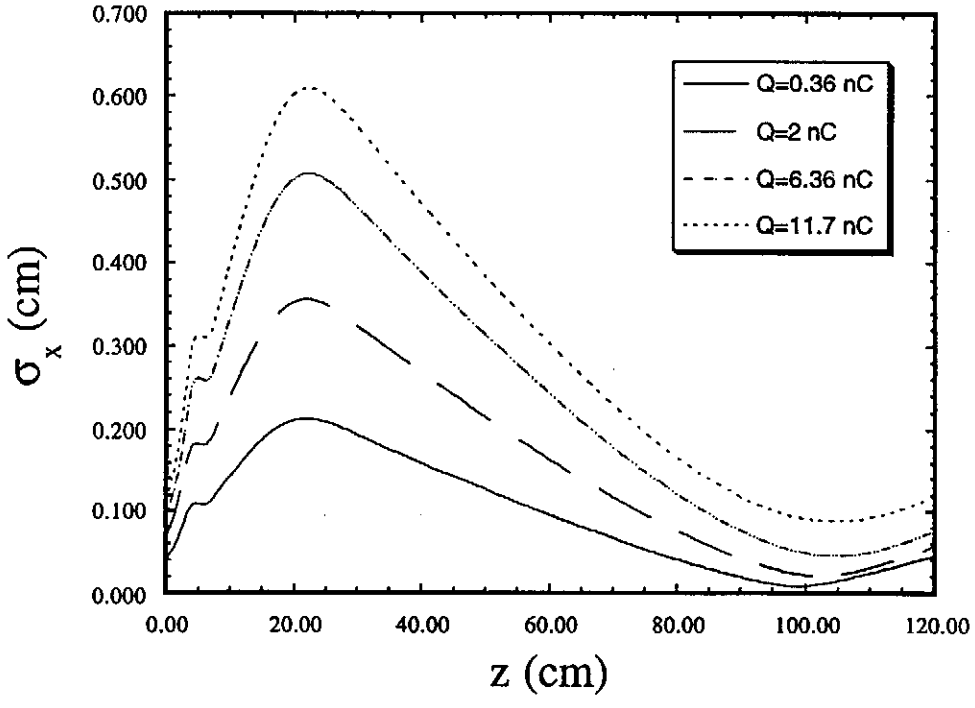


Figure 1. The evolution of the rms beam envelopes for various charge beams, following the scaling of Eq. 7, from PARMELA simulation.

The rms beam profiles for various charge beams are shown in Fig. 1. They have the same form except for a small lensing effect due to the transverse image-charge derived forces at the cathode. In addition, the evolution of the rms normalized emittance is given in Fig. 2. It is clear that the behavior of the emittance growth and compensation processes are very similar, as we expect. One striking difference is the presence of a large spike in the emittance at the gun exit (7.87 cm) in the higher charge cases, which is not present at all in the lowest charge ($Q$=0.36 nC) case. This is due to the beam size being larger in the high charge cases, which introduces rf derived emittance growth, as is discussed further below.

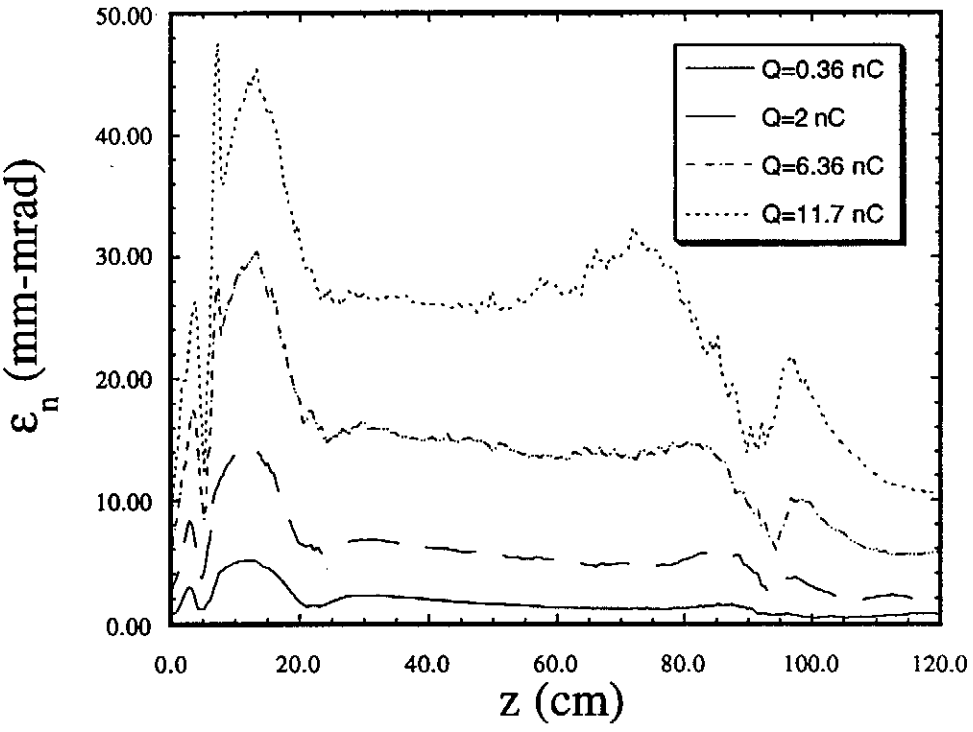


Figure 2. The evolution of the normalized rms emittance for the cases shown in Fig. 1 as a function of $z$, from PARMELA simulation.

It is now reasonable to ask a more quantitative question - how the emittance scales following this prescription for $Q$ scaling. This is not a completely simple task, as there are a number of interdependent contributions to the normalized rms emittance, defined by

$$\varepsilon_x = (m_e c)^{-1}\sqrt{\langle x^2\rangle\langle p_x^2\rangle - \langle xp_x\rangle}. \tag{8}$$

To simplify the discussion. we ignore these interdependences and treat each effect independently. To begin, we examine the dependence of the space-charge derived

emittance. This is not complicated, as all of the force integrals needed to find the rms transverse momentum will scale (including the nonlinear components of the force, but not including the cathode image-charge effects) as the beam size. Thus the space-charge derived emittance should scale as

$$\varepsilon_x^{sc} \propto \sigma_x^2 \propto Q^{2/3} \tag{9}$$

This is the same dependence that Kim[2] has deduced for the uncompensated space charge emittance for a bunch in which all dimensions are scaled together.

Another source of rms emittance is the differential focusing (as a function of longitudinal position) due to the linear transverse rf forces. This effect has been analyzed to lowest order by Kim[2], who found

$$\varepsilon_x^{rf} \approx \left(\frac{eE_0}{\sqrt{8}m_e c^2}\right)\left(k_z\sigma_z\right)^2\sigma_x^2 \propto Q^{4/3}. \tag{10}$$

The emittance again scales as the square of the transverse beam size, and additionally scales as the length of the beam squared, which is basically the lowest order variation of the cosine variation of the rf defocusing kick at the optimum exit phase from the gun. It should also be noted that there is a strong correlation between this source of emittance growth and the space-charge emittance.

A final contribution to the total rms emittance arises because of the beam's energy spread. Since this quantity increases as the square of the beam length, the possible emittance growth due to chromatic aberrations in the focusing system will increase with bunch charge. This effect scales as

$$\varepsilon_x^{ch} \propto \left(\frac{\Delta p}{p}\right)\left(\frac{\sigma_x^2}{f}\right) \propto \left(k_z\sigma_z\right)^2\sigma_x^2 \propto Q^{4/3}. \tag{11}$$

The chromatic contribution has the same scaling as linear rf emittance contribution.

The results of all of the $Q$ scaled designs is shown in Fig. 3, illustrating the effects of these sources of emittance growth combined. The asymptotic predictions of the emittance growth, that it should be (ironically) space-charge dominated at low charge ( $\varepsilon_x \propto Q^{2/3}$ ), and rf dominated ( $\varepsilon_x \propto Q^{4/3}$ ) at high charge, when the beam sizes become large, are shown, as is a simple fit to a curve which is the sum of squares of these two

asymptotic effects ( $\varepsilon_x = \sqrt{\left(aQ^{2/3}\right)^2 + \left(bQ^{4/3}\right)^2}$ ). The fit is quite good, providing support for validity of the model.

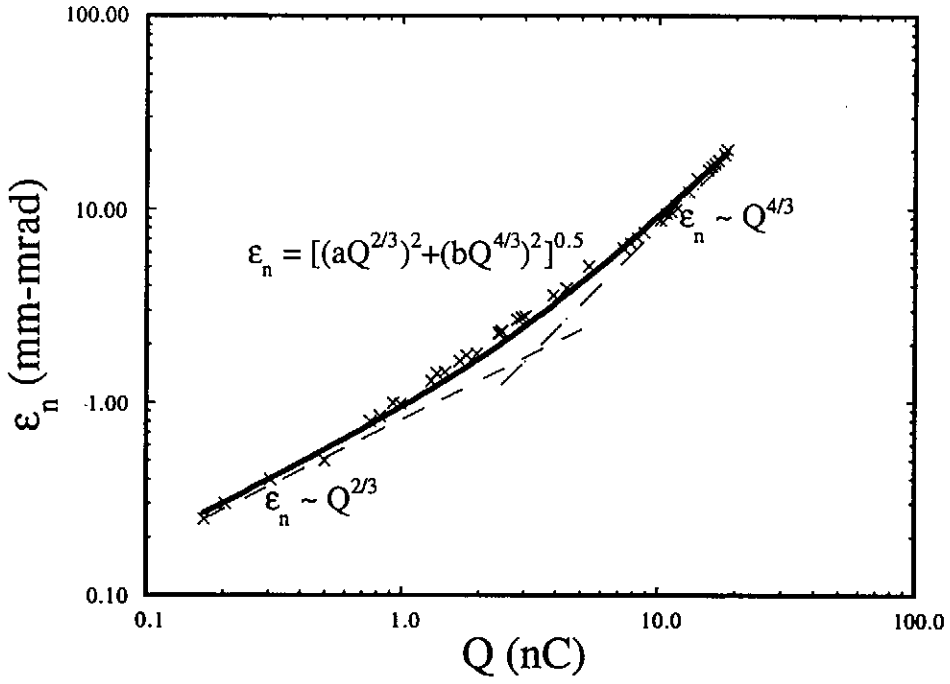


Figure 3. Normalized rms emittance as a function of charge, using the scaling of Eq. 7, from PARMELA simulation. Solid line is the fit function shown, while the dashed lines give the expected asymptotic behavior in the low and high charge limits.

## WAVELENGTH SCALING

Another situation which can arise is that one laboratory develops a sophisticated rf photoinjector design at a certain rf wavelength, and a different laboratory wishes to take advantage of this work in adapting the design to another, more convenient wavelength. This naturally brings up the question of wavelength ( $\lambda$ ) scaling of photoinjector design.

This discussion proceeds immediately from Eqs. 3 and 4, which dictate the scaling of the electric field, as mentioned before. To preserve the longitudinal motion in a design - the injection phasing, compression of longitudinal phase spread, the energies at the exit of the rf structures, etc. - one must simply follow the scaling

$$E_0 \propto \lambda^{-1}. \tag{12}$$

This course implies that the structure length is simply proportional to the rf wavelength. Further, preservation of the relative energy spread requires that the beam's injected phase spread be constant,

$$\sigma_z \propto \lambda . \tag{13}$$

For preservation of the transverse dynamics, one must scale all of the transverse wave numbers inversely with the rf wavelength, since all distances must scale with wavelength. For solenoidal focusing, this implies

$$k_{\beta,sol}^2 = \left( \frac{eB}{2\beta\gamma m_e c} \right)^2 \propto \lambda^{-2}, \tag{14}$$

which gives $B \propto \lambda^{-1}$.

For transverse rf focusing effects[2][9], we can define the effective focusing wave number in the usual way, and find

$$k_{\beta,rf}^2 \propto \frac{F_{r,rf}}{r} = \frac{e}{2}\frac{dE_z}{dz} \propto \lambda^{-2}. \tag{15}$$

Thus the transverse rf effects naturally scale correctly with wavelength if the field is inversely proportional to the wavelength.

For space charge, we recall that the aspect ratio of the beam must remain constant when scaling, and thus, because of Eq. 13, we have

$$\sigma_{x,y} \propto \lambda . \tag{16}$$

To scale the space charge defocusing wave number inversely with wavelength, from Eq. 6 we immediately deduce that

$$Q \propto \lambda . \tag{17}$$

These scaling rules have also been tested with PARMELA simulations. Figure 4 shows the evolution of the beam size for four different wavelength, properly scaled photoinjectors (scaled from a 1 nC, 2856 MHz case), with all lengths normalized to the rf wavelength. The curves lie nearly on top of each other, as the scaling rules predict.

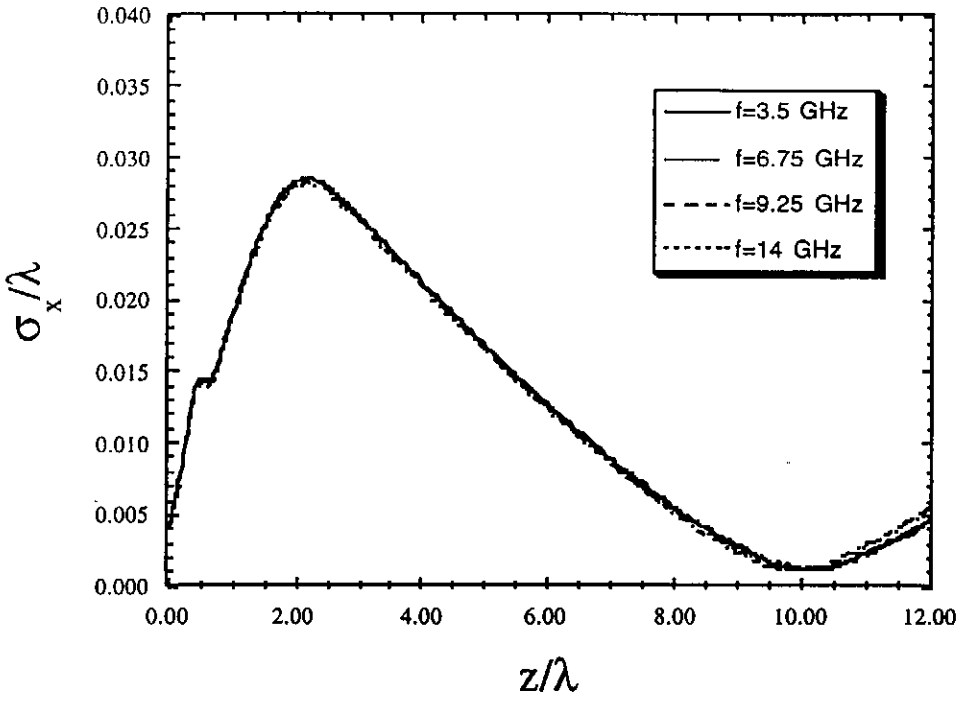


Figure 4. Rms beam size as a function of propagation distance, all lengths normalized to rf wavelength, for four different rf wavelengths in BNL-style $\lambda$ scaled photoinjector, from PARMELA simulation.

The scaling of the emittance as a function of rf wavelength is in some ways more straightforward than in the case of the charge scaling, as the result is simpler. For $\lambda$ scaling, the rms momentum integrals are proportional to the defocusing strength ($\sim \lambda^{-2}$), the beam size ($\sim \lambda$) the total rest frame integration time ($\sim \lambda$). Multiplied by the rms beam size ($\sim \lambda$), we find that

$$\varepsilon_x^{sc} \propto \lambda . \tag{18}$$

The rf contribution to the emittance scales with wavelength, from Eq. 10, as

$$\varepsilon_x^{rf} \propto E_0(k_z\sigma_z)\sigma_x^2 \propto \lambda . \tag{19}$$

The contribution to the emittance from chromatic aberrations scales as, using Eq. 11,

$$\varepsilon_x^{ch} \propto \left(\frac{\Delta p}{p}\right)\left(\frac{\sigma_x^2}{f}\right) \propto f^{-1}\left(k_z\sigma_z\right)^2\sigma_x^2 \propto \lambda . \qquad (20)$$

These results, which lead to the conclusion that the emittance is yet another "length" simply proportional to $\lambda$, is easily shown to be valid by the numerical simulations, as seen in Figs. 5 and 6.

Figure 5 is analogous to Fig. 4, showing the evolution of the emittances for the four different wavelength cases, with the propagation length and the emittance normalized to the rf wavelength. Again, the curves lie nearly on top of each other. Figure 6 shows the results of a scan of rf frequencies from 0.5 to 17.25 GHz. The scaling shown is inverse with frequency, or linear in wavelength, over this range of parameters.

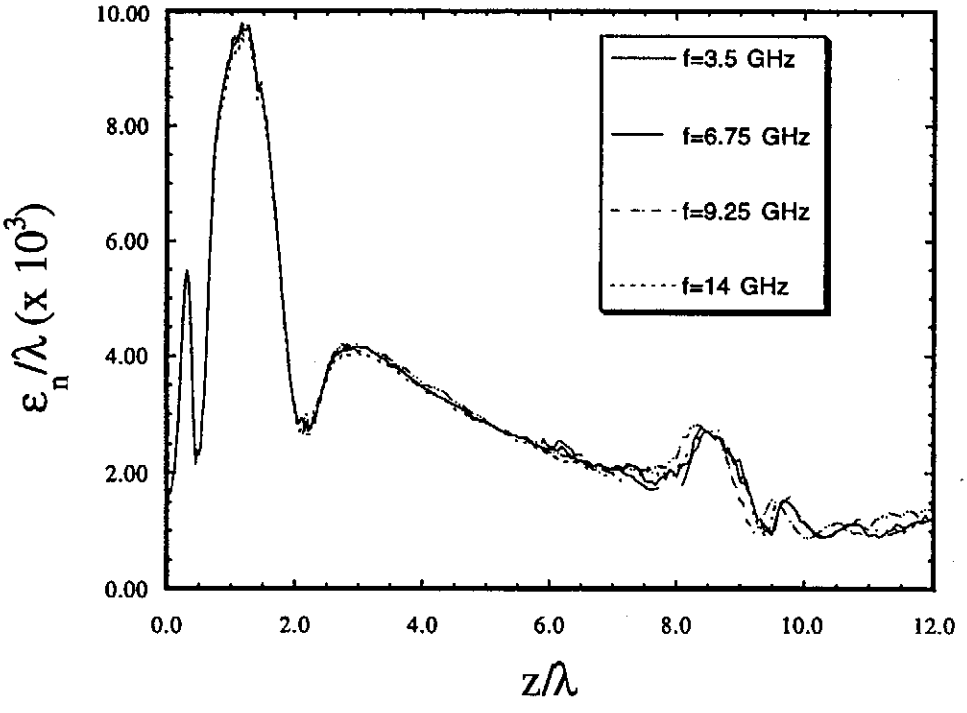


Figure 5. Emittance as a function of propagation distance, both normalized to $\lambda$, for the cases shown in Fig. 4, from PARMELA simulation.

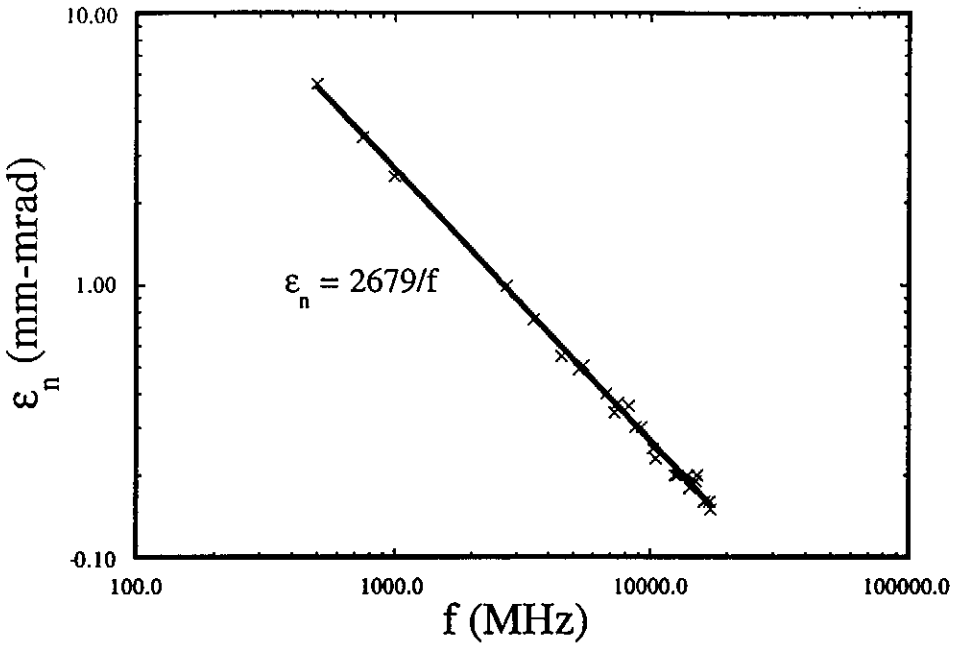


Figure 6. Normalized rms transverse emittance as a function of rf frequency, with inverse frequency dependence fit shown (solid line), from PARMELA simulation.

## DEVIATIONS FROM SCALING

The scaling laws developed in this paper work quite well over a wide range of parameter space. There are, however, some effects which do not scale as simply as those already discussed. These effects are much more worrisome in the case of $Q$ scaling. One effect that has already been mentioned is that of the space charge of the image beam at the cathode. Not only does this space charge cause a lensing effect on the beam, which was illustrated in Fig. 1, but it causes a deceleration of beam's tail particles. This effect will cause bunch lengthening and eventual cut-off of the emitted charge when the collective deceleration is equal to the applied acceleration field. The decelerating field scales with charge as follows[10-11]

$$eE_{z,sc} \propto \frac{Q}{\sigma_x^2} \propto Q^{1/3}, \tag{21}$$

and so eventually, at high charge, the longitudinal dynamics are not preserved under $Q$ scaling. On the other hand, under $\lambda$ scaling, longitudinal space charge effects scale correctly,

$$\frac{E_{z,sc}}{E_0} \propto \frac{Q}{E_0 \sigma_x^2} \propto \lambda^0, \tag{21}$$

and the longitudinal dynamics are completely preserved under $\lambda$ scaling.

In general, $\lambda$ scaling has no inherent deviations, as we have seen. Deviations from $Q$ scaling occur because the bunch dimensions are changing while the rf wavelength is not. In addition to the effects previously described, there will also be emittance growth due to the nonlinear components of the transverse rf fields, a quantitative discussion of which is beyond the scope of this paper.

## PRACTICAL CONSIDERATIONS

While $\lambda$ scaling has no inherent deviations, it has some important practical implications. The scaling of the accelerating gradient inversely with wavelength is one obvious example. In fact, because of the dynamics scaling, and practical reasons (higher gradients are supported by the structures, and peak power requirements are lower at higher rf frequencies), this scaling law is followed intuitively by most rf photoinjector designers.

The implications of $\lambda$ scaling on the applied focusing fields are perhaps not as transparent. For solenoidal focusing, $B \propto \lambda^{-1}$, while all dimensions scale as $\lambda$. This clearly implies trouble at short wavelengths, for a variety of reasons. Most prominent is that the current density in the windings must scale as

$$J_{sol} \propto \lambda^{-2}. \tag{22}$$

This is a very serious constraint. For example, in the TTF rf photoinjector design[12], the solenoid current is run at approximately two-thirds of what can be used with standard water-cooled tubing. The scaling of this 1300 MHz design to 2856 MHz would present difficulties in solenoid implementation.

Similar considerations exist for quadrupole magnets, where scaling of the focusing wave numbers requires $B' \propto \lambda^{-2}$, which implies that the pole-tip field

$$B_{\text{pole tip}} \propto \lambda^{-1}, \tag{23}$$

in analogy to the scaling of solenoidal fields.

A final difficulty in scaling to short wavelength operation is in obtaining ultra-short laser pulses and maintaining associated timing jitter tolerances.

## APPLICATION OF SCALING LAWS

Typically, if one wishes to scale an existing rf photoinjector design, both $Q$ and $\lambda$ scaling are required. Assuming one knows the desired operating wavelength and charge *a priori,* then the scaled emittance can be written

$$\varepsilon_{x,\mathrm{new}} = \left(\frac{\lambda_{\mathrm{new}}}{\lambda_{\mathrm{old}}}\right) h\left(\frac{Q_{\mathrm{new}}\lambda_{\mathrm{old}}}{Q_{\mathrm{old}}\lambda_{\mathrm{new}}}\right), \tag{24}$$

where $h$ is a normalized ($h(1)=1$) function of the design regime, *i.e.* a function like the curve fit to the data shown in Fig. 3. Assuming that one is operating within the space-charge dominated emittance region of the function, one obtains

$$\varepsilon_{x,\mathrm{new}} = \left(\frac{\lambda_{\mathrm{new}}}{\lambda_{\mathrm{old}}}\right)^{1/3}\left(\frac{Q_{\mathrm{new}}}{Q_{\mathrm{old}}}\right)^{2/3}, \quad \text{(space-charge dominant)} \tag{25}$$

and smaller emittance implies operation at smaller charge and wavelength.

In the rf/aberration dominated emittance limit, however, the scaling is changes to

$$\varepsilon_{x,\mathrm{new}} = \left(\frac{\lambda_{\mathrm{new}}}{\lambda_{\mathrm{old}}}\right)^{-1/3}\left(\frac{Q_{\mathrm{new}}}{Q_{\mathrm{old}}}\right)^{4/3}, \quad \text{(rf/aberration dominant)} \tag{26}$$

and emittance is a much more sensitive function of charge. Note that in this case operation at longer wavelength is now favored.

The most interesting of current and planned applications of rf photoinjectors is the free-electron laser (FEL). The universal gain parameter in the FEL is proportional to the gain length, which is a simple function of the beam brightness $\rho \propto L_g^{-1} \propto B_{\mathrm{beam}}^{1/3}$,

$$B_{\mathrm{beam}} = \frac{2I}{\varepsilon_x \varepsilon_y} \propto \frac{Q}{\sigma_z \varepsilon_x \varepsilon_y}. \tag{27}$$

In the space-charge dominated emittance regime, the brightness scales as

$$B_{\text{beam}} \propto \left(\frac{\lambda_{\text{old}}}{\lambda_{\text{new}}}\right)^{4/3}\left(\frac{Q_{\text{old}}}{Q_{\text{new}}}\right)^{2/3}, \quad \text{(space-charge dominant)} \quad (28)$$

and the brightness is improved by operation at longer wavelength and lower charge.

On the other hand, for the rf/aberration dominated emittance regime, we now have

$$B_{\text{beam}} \propto \left(\frac{Q_{\text{old}}}{Q_{\text{new}}}\right)^{2}, \quad \text{(rf/aberration dominant)} \quad (29)$$

and the brightness has no inherent wavelength dependence. Also, lower charge operation is quite heavily favored, even more so than in space-charge dominated emittance scaling.

These scaling laws, while interesting, need an overall normalization to be most useful. To that end, it is clear that the beam brightness also depends on having the bunch as small (placing it in the space charge dominated regime) and dense as possible in the design, and that there are limits to this density arising from space charge effects in general. Let us examine, in particular, longitudinal space charge effects, as these are inherent, and not dependent on external issues such as solenoid magnet strength. An estimation of these effects then can be employed to quantify the scaling of the beam emittance and brightness.

To proceed with this analysis, we define the aspect ratio of the beam by $\sigma_x = A\sigma_z$, as in Kim. We note at this point that emittance compensation cannot proceed with any degree of success for $A > 1$, as shorter bunches give nonlinear effects at low energy which strongly violate the assumption of self-similar forces over the entire propagation distance in the photoinjector. In addition, if we limit the maximum deceleration force on the bunch at the photocathode to one-half that of the applied rf, then we have a maximum beam density, assuming a spherically symmetric gaussian beam distribution in the laboratory frame,

$$n_b = \frac{eE_0 A}{4(2\pi)^{3/2} r_e m_e c^2 \sigma_x}. \quad (30)$$

In order to calculate brightness, we must first estimate the in emittance. We have already written Kim's estimate of the rf emittance, and we must do the same for the compensated space charge emittance. For this, we take Kim's estimate for the space-charge emittance, and lower it by one order of magnitude. This *ansatz* is well motivated by empirical observation of simulation and experiment, and by the fact that the emittance must scale as

such, since Kim's estimate gives the correct scaling of the strength of the space charge forces. Thus we estimate

$$\varepsilon_x^{sc} \approx \frac{m_e c^2}{(2\pi)^2 e E_0} \frac{I}{I_0(1+\frac{3}{5}A)} \approx \frac{\sigma_z}{4(2\pi)^{5/2}} \frac{A^2}{1+\frac{3}{5}A}, \tag{31}$$

which is in excellent quantitative agreement with the PARMELA simulation results shown in Fig. 3. It is important to restate that the explicit scaling of the middle expression is the same as the prediction of our $Q$ scaling analysis ($\varepsilon \propto I \propto Q^{2/3}$), while the right hand expression has "incorrect" explicit scaling, because of absorbing the current dependence on the applied field. In other words, the scaling of the right hand expression in Eq. 31 has implicit rf field dependence, and therefore is not simple $Q$ scaling.

Given Eqs. 10, 30 and 31, and ignoring the chromatic aberration emittance, we now can write an expression for the beam brightness in terms of the applied field and the bunch length

$$B \approx \left[ \left( \frac{m_e c^2}{8(2\pi)^5 e E_0 \sigma_z} \right) \left( \frac{A^2}{1+\frac{3}{5}A} \right)^2 + \left( \frac{e E_0 \sigma_z}{4 m_e c^2} \right) \left( \frac{\delta p}{p} \right)^2 \right]^{-1} \frac{A^2 I_0}{\sqrt{2\pi}\sigma_z^2}, \tag{32}$$

where we have substituted the momentum spread at optimum injection phase $\delta p/p = (k_z \sigma_z)^2/2$. Once the momentum spread is chosen to be a reasonable value (we take 1%) to mitigate chromatic aberrations, the quantity $E_0 \sigma_z \propto k_z \sigma_z$ (for a given value of $\alpha$) is also chosen. Also, in practice, one finds not much deviation from $\alpha \approx 1.5$ after optimization of beam dynamics. Also, it is straightforward to show that for any reasonable choice of the momentum spread that the second term in the brackets (the rf emittance term) is ignorably small, as it must be in this regime. In any case, it could have been previously deduced from Eqs. 28 and 29 that one should indeed operate in the space charge dominated emittance regime, and therefore the maximum brightness one can achieve out of an rf photoinjector is approximately

$$B \approx 16(2\pi)^{9/2} \alpha k_z \sigma_z \frac{I_0}{\sigma_z^2} \frac{(1+\frac{3}{5}A)^2}{A^2} \approx 2.9 \times 10^{10} \frac{\alpha}{\sqrt{\frac{\delta p}{p}}\lambda^2} \frac{(1+\frac{3}{5}A)^2}{A^2} \text{ (A/m2)}, \tag{33}$$

under the assumptions that the beam is a cylindrically symmetric gaussian. As a check we note that the present design for the BNL upgraded gun calls for a peak current of 100 A,

$A = 0.6$, $\alpha = 1.63$, $\delta p/p = 5 \times 10^{-3}$ and an emittance of 1 mm-mrad, giving a brightness of $B \approx 2 \times 10^{14}$ A/m$^2$, while Eq. 33 yields $B = 2.7 \times 10^{14}$ A/m$^2$, which is remarkably good agreement, considering the approximations used in our derivation.

## CONCLUSIONS

The correct method for scaling of rf photoinjector designs with charge and wavelength has been explored in detail, and scaling laws for emittance and brightness have been developed in the process. The scaling methods should prove most useful for rf photoinjector designers who wish to make use of existing mature designs, especially in achieving emittance compensation with a minimum of computational effort.

Both the qualitative and quantitative discussion of emittance and brightness provided in the last section points to small beam sizes and rf wavelengths for improved performance. These conclusions should be tempered by several considerations. First, many applications in FEL and linear colliders demand a certain beam charge or power for their specific application in addition to brightness or emittance requirements. Also, shorter wavelength operation presents technical difficulties which may be insurmountable for a given scaled design, as mentioned above. These technical questions are not being addressed widely in the rf photoinjector community, as there is only one rf photoinjector project at a wavelength shorter than S-band, the 17 GHz rf gun at MIT[13]. This project provides interesting challenges which should illuminate the issue of short wavelength, small bunch ultra-high brightness operation.

## ACKNOWLEDGMENTS

This work performed with partial support from U.S. Dept. of Energy grants DE-FG03-90ER40796 and DE-FG03-92ER40693, and the Alfred P. Sloan Foundation grant BR-3225.

## REFERENCES

1. J. Fraser, *et al., IEEE Trans. Nucl. Science* **NS-32**, 1791 (1985).
2. K.J.Kim, *Nucl. Instr. Methods A* **275**, 201 (1988).
3. B.E. Carlsten, *Nucl. Instr. Methods A* **285**, 313 (1989).
4. J.C. Gallardo and H. Kirk, *Proc. Particle 1993 Accel. Conf.* 3615 (IEEE, 1993).
5. R. Sheffield, *et al., Nucl. Instr. Methods A* **341**, 371 (1994).
6. L. Serafini, *Nucl. Instr. Methods A* **340**, 40 (1994).
7. P. Lapostolle, *Proton Linear Accelerators : A Theoretical and Historical Introduction* (LA-11601-MS, Los Alamos, 1989).
8. J.B. Rosenzweig, *et al.,* in the *Proc. Particle 1993 Accel. Conf.,* 3021 (IEEE, 1993).
9. J.B. Rosenzweig and L.Serafini, *Phys.Rev.E* **49**, 1499 (1994) and S.C. Hartman and J.B. Rosenzweig, *Phys. Rev. E* **47**, 2031 (1993).
10. J.B. Rosenzweig, *et al., Nucl. Instr. Methods A* **341**, 379 (1994).
11. C. Travier, *et al., Nucl. Instr. Methods A* **340**, 26 (1994).
12. E. Colby, J.B. Rosenzweig and J.F. Ostiguy, these proceedings.
13. S.C.Chen, *et al.,* in the *Proc. Particle 1993 Accel. Conf.,* 2575 (IEEE, 1993).